


RESEARCH

Open Access



# Dichotomous role of Shp2 for naïve and primed pluripotency maintenance in embryonic stem cells

Seong-Min Kim<sup>1</sup>, Eun-Ji Kwon<sup>1</sup>, Yun-Jeong Kim<sup>1</sup>, Young-Hyun Go<sup>2</sup>, Ji-Young Oh<sup>1</sup>, Seokwoo Park<sup>3</sup>, Jeong Tae Do<sup>4</sup>, Keun-Tae Kim<sup>1,2\*</sup> and Hyuk-Jin Cha<sup>1,2\*</sup> 

## Abstract

**Background:** The requirement of the Mek1 inhibitor (iMek1) during naïve pluripotency maintenance results from the activation of the Mek1-Erk1/2 (Mek/Erk) signaling pathway upon leukemia inhibitory factor (LIF) stimulation.

**Methods:** Through a meta-analysis of previous genome-wide screening for negative regulators of naïve pluripotency, *Ptpn11* (encoding the Shp2 protein, which serves both as a tyrosine phosphatase and putative adapter), was predicted as one of the key factors for the negative modulation of naïve pluripotency through LIF-dependent Jak/Stat3 signaling. Using an isogenic pair of naïve and primed mouse embryonic stem cells (mESCs), we demonstrated the differential role of Shp2 in naïve and primed pluripotency.

**Results:** Loss of Shp2 increased naïve pluripotency by promoting Jak/Stat3 signaling and disturbed *in vivo* differentiation potential. In sharp contrast, Shp2 depletion significantly impeded the self-renewal of ESCs under primed culture conditions, which was concurrent with a reduction in Mek/Erk signaling. Similarly, upon treatment with an allosteric Shp2 inhibitor (iShp2), the cells sustained Stat3 phosphorylation and decoupled Mek/Erk signaling, thus iShp2 can replace the use of iMek1 for maintenance of naïve ESCs.

**Conclusions:** Taken together, our findings highlight the differential roles of Shp2 in naïve and primed pluripotency and propose the usage of iShp2 instead of iMek1 for the efficient maintenance and establishment of naïve pluripotency.

**Keywords:** *Ptpn11*, Shp2, Tyrosine phosphatase, Naïve pluripotency, Self-renewal, Mek1, 2i/LIF, Embryonic stem cells, Primed pluripotency, Erk1/2

## Background

Although mouse embryonic stem cells (mESCs) have been widely used to characterize the early embryonic development of mammals, these cells exhibit clear differences from human ESCs at the cellular (e.g., colony morphology and surface markers) [1] and molecular

levels, such as different epigenetic states, X-chromosome inactivation, chimera formation, major signaling pathways [2, 3], and glucose metabolism [4], among others [5]. Based on recent advances in our understanding of pluripotency, two discrete pluripotent states, naïve (or ground) and primed, have been recognized. In more detail, “naïve” and “primed” cells represent the peri-implanted blastocyst, at E4.5 and post-implanted embryo (from E5.5 onwards) [6]. Since naïve ESCs are established from human ESCs [7], dissimilarities of human to mouse

\*Correspondence: keuntaekim91@gmail.com; hjcha93@snu.ac.kr

<sup>1</sup> College of Pharmacy, Seoul National University, 1 Gwanak-ro Gwanak-gu, Seoul 08826, Republic of Korea

Full list of author information is available at the end of the article



© The Author(s) 2022. **Open Access** This article is licensed under a Creative Commons Attribution 4.0 International License, which permits use, sharing, adaptation, distribution and reproduction in any medium or format, as long as you give appropriate credit to the original author(s) and the source, provide a link to the Creative Commons licence, and indicate if changes were made. The images or other third party material in this article are included in the article's Creative Commons licence, unless indicated otherwise in a credit line to the material. If material is not included in the article's Creative Commons licence and your intended use is not permitted by statutory regulation or exceeds the permitted use, you will need to obtain permission directly from the copyright holder. To view a copy of this licence, visit <http://creativecommons.org/licenses/by/4.0/>. The Creative Commons Public Domain Dedication waiver (<http://creativecommons.org/publicdomain/zero/1.0/>) applies to the data made available in this article, unless otherwise stated in a credit line to the data.

ESCs have been explained to be unique characteristics of primed pluripotency [8].

A constant supply of leukemia inhibitory factor (LIF) along with two chemical inhibitors for Mek1 (iMek1) and Gsk3 $\beta$  (iGsk3 $\beta$ ) (hereinafter referred to as LIF + 2i) is indispensable [9] not only for maintenance but also for the establishment of naïve ESCs, thus mimicking the characteristics of naïve pluripotency of pre-implantation embryos in vitro. LIF-mediated propagation and maintenance of naïve ESCs depend on the Jak/Stat3 pathway [10], which is also conserved in embryo development and implantation [11]. Two inhibitors are required for maintaining naïve pluripotency, which is likely attributed to the innate mechanism of Gsk3 $\alpha/\beta$  inhibition in the inner cell mass (ICM) of blastocysts [12] coupled with a lower basal activity of Erk1/2 (hereinafter Erk) in early blastocysts [13], the latter of which is possibly due to the expression of Erk-specific dual-specificity phosphatases (DUSPs) [14, 15].

Src homology region 2 domain-containing phosphatase 2 (Shp2), which is encoded by protein tyrosine phosphatase non-receptor type 11 (*Ptpn11*), transmits the receptor signaling to Erk [16] and negatively modulates Jak/Stat3 signaling [17]. Phosphorylation of Shp2 upon cytokine stimulation by interleukin-6 (IL-6) or LIF, leads to intramolecular conformational changes to relieve autoinhibition of tyrosine phosphatase activity [18] and dephosphorylates the Jak/Stat3 pathway [18, 19]. In parallel, the recruitment of phosphorylated Shp2 to gp130 forms a protein complex with Gab1 to transduce signals from the receptor to Ras/Raf/Mek/Erk [20]. Considering the positive role of Shp2 in Ras-dependent Erk activation (Ras-to-Erk), as well as in oncogenic Ras-to-Erk [21, 22] and target therapy resistance [23], small molecules to inhibit the bivalent roles of Shp2 have been developed as novel anti-cancer therapeutic agents [24].

As negative roles of Shp2 in self-renewal of mESCs through Erk [25], Shp2 deficiencies promote self-renewal capacity and suppress mESC differentiation through increased sensitivity to LIF on Jak/Stat3 and attenuation of Ras-to-Erk [17]. Similarly, failure to recruit Shp2 [26] and Shp1 [2] to the site of Stat3 activation sensitizes mESCs to LIF in the Jak/Stat3 signaling pathway, thus favoring self-renewal. In contrast, the molecular mechanisms that control the pluripotency and differentiation of hESCs via SHP2 depletion are different from those of mESCs [27], which suggests the dichotomous role of Shp2 in naïve and primed ESCs.

Here, we demonstrated that transient activation of Shp2 by LIF negatively modulated Jak/Stat3 signaling and transmitted the signal to Ras-to-Erk, which consequently resulted in an attenuation of naïve pluripotency. Accordingly, depletion of Shp2 or iShp2 (a chemical inhibitor of

Shp2) treatment favors naïve pluripotency by sensitizing the Jak/Stat3 signaling pathway to LIF stimulation and decoupling Ras-to-Erk signaling, whereas primed ESCs were intolerant to Shp2 perturbation. The dichotomous effect of Shp2 inhibition thus favored the enrichment of naïve ESCs. Additionally, iShp2 could efficiently substitute iMek1 for the maintenance and establishment of naïve pluripotency.

## Results

### Shp2 activation by LIF negatively affects naïve pluripotency

Upon LIF stimulation following LIF deprivation, we observed that Erk activation occurred along with Stat3 phosphorylation (Fig. 1A). To determine the occurrence of naïve pluripotency, we took advantage of OG2 mESCs, which express naïve specific green fluorescent protein (GFP) under the control of the Oct4 promoter due to the lack of a proximal enhancer [28, 29]. Consistent with previous reports [6], a lack of 2i resulted in the loss of the dome shape that characterizes naïve specific colony morphology (Additional file 1: Fig. S1A, Additional file 2: Movie S1A, Additional file 3: Movie S1B, Additional file 4: Movie S1C) and significantly attenuated GFP signals even under LIF stimulation (Fig. 1B). Due to innate negative regulator(s) toward Stat3 [30], Stat3 phosphorylation after LIF stimulation (Fig. 1A) and its transcriptional activity (Additional file 1: Fig. S1B) were attenuated along with Erk activation through a series of protein interactions. Therefore, the putative negative feedback mechanism(s) and/or Erk activation upon LIF stimulation, would be responsible for the constant supply of LIF + 2i for maintaining naïve pluripotency. In a previous study, genome-wide CRISPR screening identified a set of negative and positive regulators of naïve pluripotency [31]. A total of 155 genes (Additional file 1: Fig. S1C and Additional file 9: Table S1), whose perturbation significantly affected naïve pluripotency [31], were examined via gene ontology (GO) and KEGG pathway analysis. As expected, based on the significance of LIF-mediated signaling on naïve pluripotency described in other studies, these 155 genes were highly enriched in several associated pathways including 'Interleukin-6 signaling', 'Jak/Stat3 signaling', and 'PluriNetWork' (Additional file 1: Fig. S1D). Particularly, a few genes among a set of 27 positive regulators (shown in red) and 128 negative regulators (shown in blue) were associated with the 'Naïve pluripotency signaling' (Additional file 1: Fig. S1E), 'JAK/STAT signaling' (Additional file 1: Fig. S1F), and 'Ras signaling' (Additional file 1: Fig. S1G) pathways. Among 27 putative negative regulators, three genes including *Grb2*, *Ptpn2*, and *Ptpn11* belonged to



**Table 1** Sequences of primers for quantitative real-time PCR

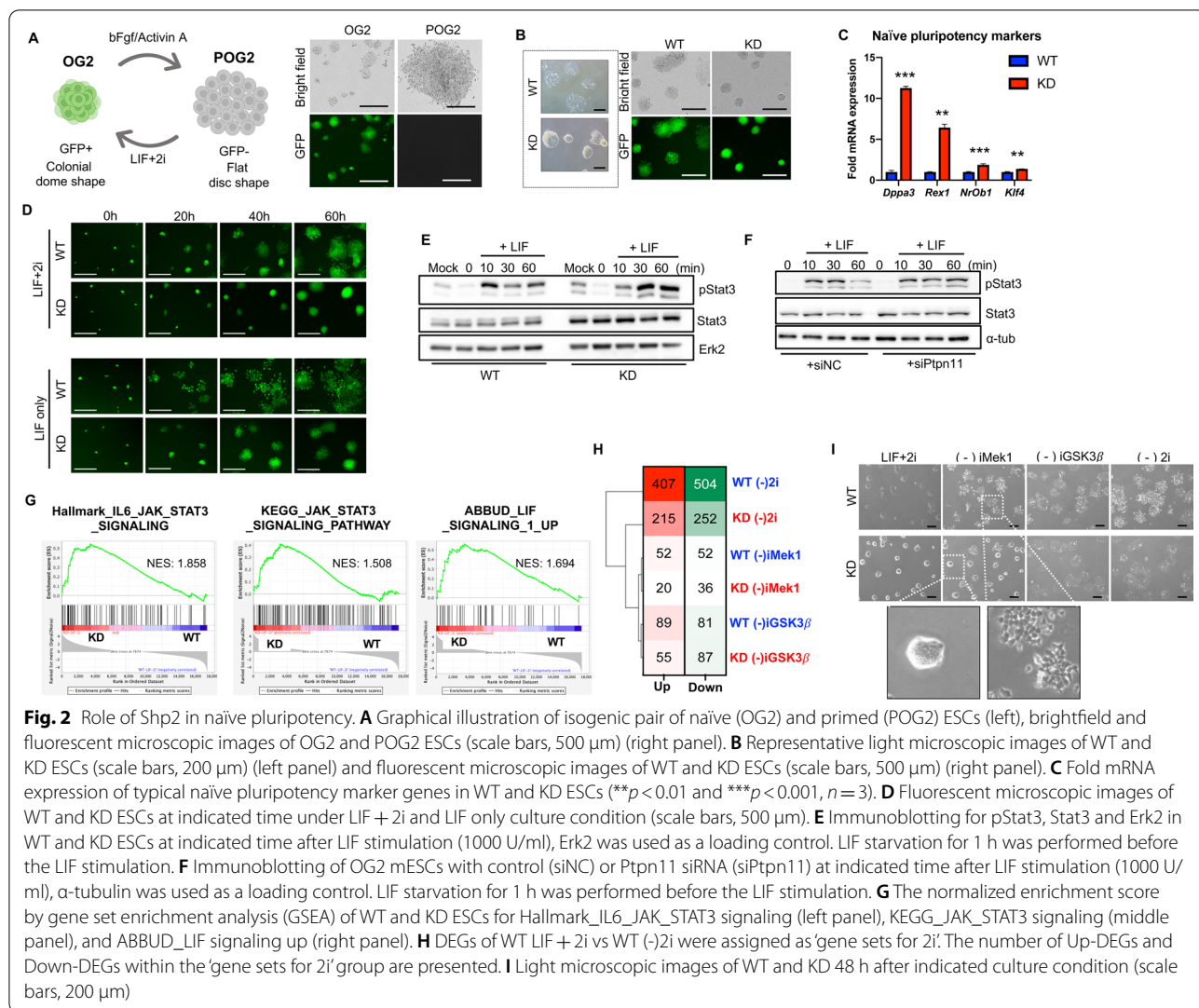
Primer pairs		Primer sequences (5'-3')
Ptpn11	Forward	AGTCCAAAGTGACCCACGTC
	Reverse	CCATCATGCAGAACGACCTT
Dppa3	Forward	CGTACCTGTGGAGAACAAGAGTG
	Reverse	CA TTCTCAGAGGGA TCCCA TCTTTG
Rex1	Forward	CTTCGAAAGCTTGGAGGAAGTGAG
	Reverse	GGACACTCCAGCATCGATAAGACAC
Nr0b1	Forward	ACAGAGCAGCCACAGA TGGTGTC
	Reverse	GATGTGCTCAGTAAGGATCTGCTG
Klf4	Forward	GAACAGCCACCCACACTTGTGAC
	Reverse	CTGTCACTTCTGGCACTGAAAG
Esrrb	Forward	GATTCTCATCTTGGGCATCGTGAC
	Reverse	CTGACTCAGCTCATAGTCTGCAG
Klf2	Forward	CACACATACTGCAGCTACACCAAC
	Reverse	CAAGTGGCACTGAAAGGTTCTGTG
Fgf5	Forward	CATCGGTTTCCATCTGCAGACTAC
	Reverse	GTTCTGTGGATCGCGGACGCATAG
Cer1	Forward	GTGGAAAGCGA TCA TGTCTCA TCG
	Reverse	GCAAAGGTTGTCTGGACAACGAC
Pou5f1	Forward	GAGAAAGCGAACTAGCATTGAGAAC
	Reverse	TGTAGCCTCATACTTCTCTCGTTG
Sox2	Forward	ATGGGCTCTGTGGTCAAGTC
	Reverse	CCCTCCCAATCCCTTGTAT
Nanog	Forward	GTGCACTCAAGGACAGGTTTTCAG
	Reverse	CTGCAATGGATGCTGGGATACTC
c-Myc	Forward	ACCACCAGCAGCGACTCTGA
	Reverse	TGCCTCTTCTCCACAGACACC

the “IL-6/JAK/STAT signaling” pathway according to MSigDB Hallmark 2020 (<https://maayanlab.cloud/Enrichr/>) [32] (Fig. 1C). We next focused on *Ptpn11*, which encodes the Shp2 protein that dephosphorylates Stat3, thus acting as an important negative regulator of IL-6 stimulation [33], and transduces signals toward Ras-to-Erk possibly through Grb2 [34]. Considering the close similarity between LIF and IL-6 [35], we presumed that the activation of Shp2 by LIF would act as a negative regulator on naïve pluripotency by Stat3 dephosphorylation and Erk1/2 activation. As predicted, active phosphorylation of Shp2 (Y542) occurred promptly after LIF stimulation in parallel with signal transduction to Ras-to-Erk (Fig. 1D), thus relieving its auto-inhibitory regulation on phosphatase activity [18]. In parallel with Shp2 active phosphorylation (Fig. 1D), the phosphatase activity of Shp2 [about 45% inhibited by Shp2 inhibitor (iShp2) treatment], was also clearly induced by LIF stimulation (about 60% increased) (Fig. 1F). These data suggest that Shp2 activation by LIF simultaneously controls both Jak/Stat3 and Ras-to-Erk signaling to affect naïve pluripotency (Fig. 1G).

### Role of Shp2 in naïve pluripotency

Although the roles of Shp2 were well-characterized in self-renewal of mESCs with knockdown (KD) or knockout (KO) models [17], we noticed that the effect of Shp2 in human ESCs (hESCs) was less evident than that of mESCs [27]. Given that hESCs share the molecular and cellular characteristics of primed ESCs [8], we hypothesized that the effect of Shp2 in naïve pluripotency would differ from that of primed pluripotency. To evaluate this hypothesis, we utilized the isogenic model of pair of primed ESCs (P-OG2) and naïve ESCs (OG2). As previously described [29], naïve ESCs with a ‘colonial dome shape’ exhibit GFP signals unlike primed ESCs, which exhibit a ‘flat disc shape’ (Fig. 2A), expressing typical marker genes of the naïve and primed state (Additional file 1:Fig. S2A and B). Stable knockdown of *Ptpn11* was performed using a pair of naïve and primed ESCs. As expected, based on previous studies performed in mESCs, naïve ESCs with clear *Ptpn11* knockdown (hereinafter referred to as Shp2 KD or KD naïve ESCs) (Additional file 1:Fig. S2C) exhibited a clear ‘colonial dome shape’ with an increased GFP signal (Fig. 2B). Consistently, naïve cell-specific marker genes were also significantly enhanced in KD Naïve ESCs (Fig. 2C), whereas core pluripotency genes only exhibited marginal changes (Additional file 1:Fig. S2D). Interestingly, KD Naïve ESCs maintained a stable GFP signal even under LIF treatment without 2i supplement (LIF only), which significantly affected the aforementioned ‘colonial dome shape’ morphology (Additional file 1:Fig. S2E) as well as the GFP signal of wild-type (WT) cells (Fig. 3D). Based on the drastic increase in active phosphorylation and phosphatase activity (Fig. 1D and E) of Shp2 by LIF, the prolonged naïve characteristics of KD naïve ESCs under the LIF-only condition resulted from sustained Stat3 phosphorylation via stable (Fig. 2E) and transient (Fig. 2F) Shp2 depletion. These results were also supported by the gene set enrichment analysis (GSEA) [36] of FPKM values from the WT and KD transcriptomes. Consistently, the gene set for ‘Hallmark IL6 JAK STAT3 signaling’, ‘KEGG JAK STAT3 signaling pathway’, and ‘LIF signaling 1 UP’ were significantly enriched in the KD cells compared to their WT counterparts (Fig. 2G). However, we still could not fully account for the marginal effect of 2i withdrawal on GFP signals (Fig. 2D and Additional file 5: Movie S2A, Additional file 6: Movie S2B, Additional file 7: Movie S2C, Additional file 8: Movie S2D), as well as the morphological changes of KD, illustrated in Additional file 1:Fig. S2E. Therefore, the transcriptomes of WT and KD naïve ESCs after depletion of iMek1 or iGsk3 $\beta$  were analyzed next. Compared to the transcriptome of LIF + 2i, the WT





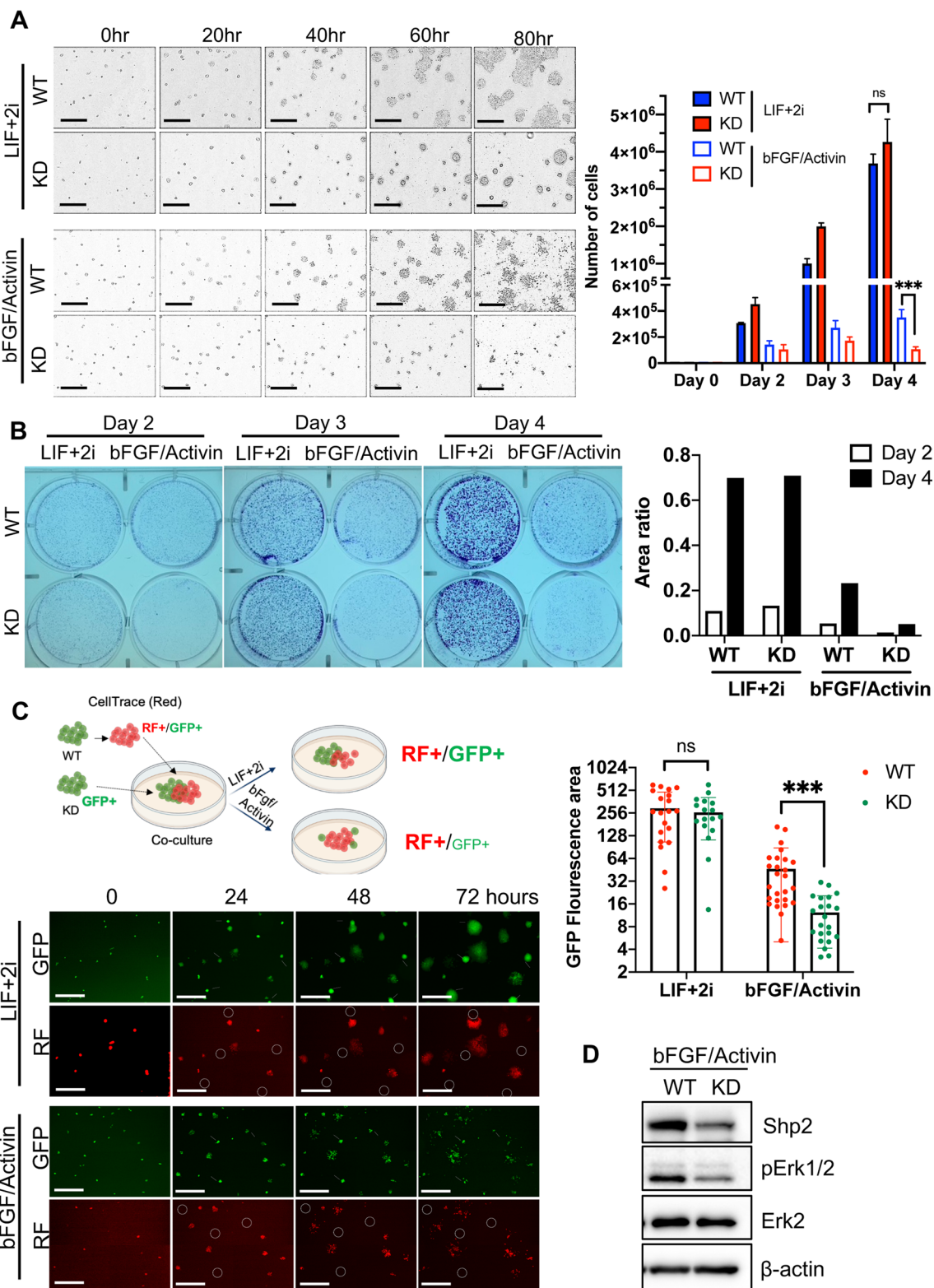
(See figure on next page.)

**Fig. 3** Role of Shp2 in primed pluripotency. **A** Light microscopic images of WT and KD ESCs at indicated times under LIF + 2i or bFGF/Activin culture condition (scale bars, 500 μm) (left), Graphical presentation of cell number at indicated time after seeding of 1 × 10<sup>4</sup> ESCs (right). **B** Images of clonogenic assay of WT and KD ESCs at indicated time under LIF + 2i or bFGF/Activin culture condition (left), Graphical presentation of area ratio (A.U.) of clones at day 2 and day 4 determined by ImageJ (right). **C** Graphical illustration of competition assay with WT, labeled with red fluorescence [RF/GFP], and KD [GFP only] mESCs (top), Fluorescence microscopic images of WT or KD ESCs at indicated time after each culture condition, circles indicate KD ESCs [GFP only] (scale bars, 500 μm) (left), Relative fluorescence intensity of WT (red) and KD (green) ESCs from GFP images from 72 h was presented as a graph (right) (\*\*\*p < 0.001, n = 26). **D** Immunoblotting analysis of WT and KD ESCs grown under bFGF/Activin for Shp2, pStat3, pErk1/2, Erk2 and β-actin. β-actin was used as a loading control

transcriptome lacking 2i (WT LIF only) exhibited the largest number of DEGs, thus manifesting the most severe alterations. Therefore, to compare the effect of depletion of each inhibitor, ‘WT LIF only’ DEGs were designated as ‘gene sets for 2i’ for comparison. Within the ‘gene sets for 2i’, KD naive ESCs lacking iMek1 [KD (-) iMek1] were altered the least (Fig. 2H) compared to

the other cells, suggesting that KD naive ESCs would be more tolerant to iMek1 depletion.

As predicted, unlike WT cells, the ‘colonial dome shape’ morphology of KD naive ESCs remained unaltered without iMek1 supplementation but was quickly lost after iGsk3β withdrawal (Fig. 2I). Given that Shp2 has another role as a signal transducer to Ras-to-Erk in addition to



tyrosine phosphatase, a lack of Shp2 may decouple the signal transduction to Erk upon LIF stimulation. Consistent with the results in Fig. 2G and H, phosphorylated Mek1 and Erk (Additional file 1:Fig. S2F) was attenuated in KD naïve ESCs, whereas no clear alteration in GSK3 $\beta$  phosphorylation was observed (Additional file 1:Fig. S2G). These data were also supported by GSEA, showing that the gene signatures of “Hallmark KRAS signaling DN and UP” were more enriched in KD naïve ESCs when iMek1 was depleted (Additional file 1:Fig. S2H).

### Role of Shp2 in primed pluripotency

Unlike naïve ESCs, primed ESCs were likely intolerant to the absence of Shp2. Despite multiple trials, the establishment of primed ESCs with stable Shp2 depletion was unsuccessful due to the severe growth retardation of primed ESCs after Shp2 knockdown (Additional file 1:Fig. S3). Alternatively, KD naïve ESCs were subjected to primed culture conditions (with bFGF/Activin) to establish KD primed-like ESCs. Although KD naïve ESCs propagated well in naïve culture conditions, they did not successfully grow in primed culture conditions (Fig. 3A and Additional file 10: Movie S3A, Additional file 11: Movie S3B, Additional file 12: Movie S3C, Additional file 13: Movie S3D). This dichotomous effect of Shp2 depletion on primed ESCs compared to naïve ESCs was further highlighted by clonogenic assays (Fig. 3B), which account for prompt culling of KD ESCs (labeled with GFP only) from the WT ESCs (labeled with RF/GFP) mixture under primed conditions unlike naïve conditions (Fig. 3C and Additional file 14: Movie S4A, Additional file 15: Movie S4B). As similar as that of naïve ESCs, signaling to Erk upon bFGF/Activin stimulation was markedly attenuated in KD ESCs (Fig. 3D). These results indicate that the self-renewal of primed ESCs depends on Shp2-dependent signaling unlike that of naïve ESCs.

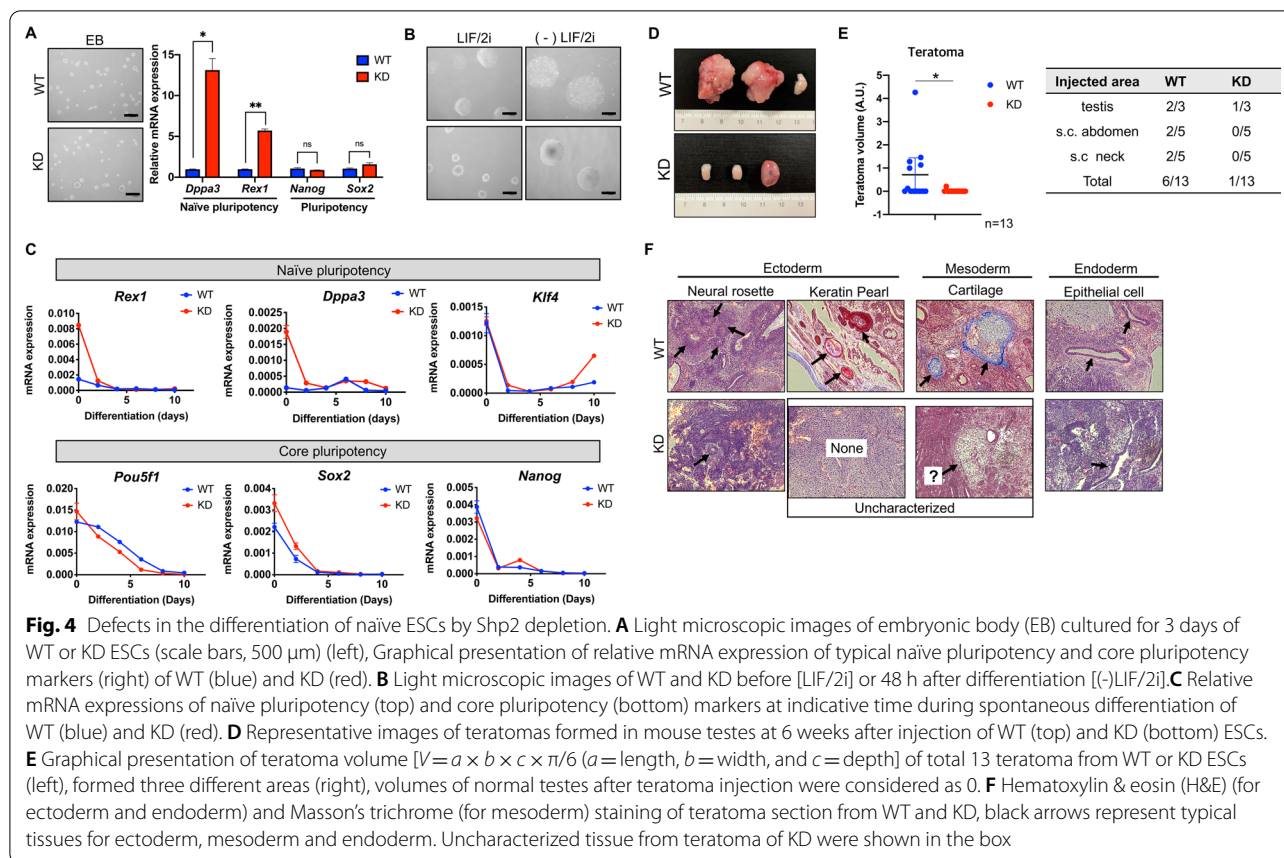
### Defects in the differentiation of naïve ESCs by Shp2 depletion

Shp2 null mice failed to develop as a result of peri-implantation lethality, which is caused by trophoblast failure [37]. Similar to the high bFGF signaling dependence described above, trophoblast stem cells (TS) and epiblast stem cells (EpiSCs), which share a close similarity to primed ESCs, rely on bFGF signaling [38]. As previously proposed [37], embryo development failure in Shp2 null mice may result from defects in the transition from naïve to primed ESCs in accordance with the TS impediment. Naïve ESCs after Shp2 depletion tended not only to maintain naïve pluripotency (Fig. 2) but also to hinder the progression to primed ESCs (Fig. 3), and therefore the differentiation potential of KD naïve ESCs

would be disturbed. Thus, WT and KD naïve ESCs were subjected to spontaneous differentiation via LIF/2i withdrawal from embryoid body (EB) formation (Fig. 4A). During spontaneous differentiation, which initiates with EB formation, typical marker genes of naïve pluripotency were clearly upregulated in the embryoid bodies of KD naïve ESCs (Fig. 4A). Along with different EB morphology (Fig. 4B), naïve pluripotency genes remained marginally high one day after differentiation induction and sharply suppressed when core pluripotency marker genes were similarly repressed (Fig. 4C). Thus, spontaneous differentiation was enforced with the serum-induced exit from naïve pluripotency regardless of Shp2. However, unlike in vitro differentiation, the formation of teratoma from KD naïve ESCs was significantly impaired in multiple sites compared to those from WT (Fig. 4D). One teratoma-like mass that was formed out of a total of 13 injections of KD naïve ESCs (Fig. 4E) only exhibited a few ectoderm and endoderm tissue structures without clear mesoderm tissue formation, unlike the well-developed teratoma from WT (Fig. 4F). It is also worth noting that Shp2 is required for proper gastrulation and mesoderm patterning in mouse [39] and *Xenopus* [40] development.

### Shp2 chemical inhibitor as an iMek1 replacement

There is emerging evidence that Shp2 contributes to chemoresistance and cancer development [21, 22, 41], and therefore Shp2 allosteric inhibitors that interfere in both phosphatase and signal transduction have been developed as novel anti-cancer therapeutic agents [21]. We first examined whether an allosteric Shp2 inhibitor (Fig. 5A, RMC-4550: iShp2), which was initially developed to decouple the oncogenic Ras-to-Erk signaling in human cancers [21], inhibits LIF-dependent Erk activation. At an iShp2 concentration known to decrease the basal level of Erk2 phosphorylation (Fig. 5B), Stat3 phosphorylation was significantly sustained after LIF stimulation in naïve ESCs (Fig. 5C), which was associated with higher Stat3 reporter activity in the presence of iShp2 8 h after LIF deprivation (Fig. 5D). Additionally, iShp2 treatment also preserved Stat3 phosphorylation even at a 1/100-fold LIF concentration (Fig. 5E) and markedly rescued naïve ESCs from cell death at a low LIF concentration (Fig. 5F). Similar to our observations in KD naïve ESCs (Fig. 2I), iShp2 treatment could likely replace the effects of iMek1 (but not iGSK3 $\beta$ ) on the ‘colonial dome shape’ morphology of naïve ESCs (Fig. 5G), which may result from the clear decoupling of LIF mediated Ras-to-Erk signaling by iShp2 treatment (Fig. 5C). Similarly, typical naïve marker genes (Fig. 5H) and the GFP signal (Fig. 5I) indicated that iShp2 treatment compensated for the loss of iMek1 in naïve ESCs. Next to validate the dichotomous effect of iShp2 in naïve



and primed ESCs, we took advantage of mESCs expressing GFP and/or RFP due to distinct enhancer activity of *Pou5f1* (encoding Oct4) in naïve (or ICM) [under control of distal enhancer (DE)] and primed (or epiblast) [under control of proximal enhancer (PE)] ESCs [42] (Fig. 5J). As illustrated in Fig. 5J, while ESCs of intermediate status expressing both GFP and RFP proliferate under LIF only condition (Fig. 5J), naïve (e.g., GFP + only) and primed (e.g., RFP + only) ESCs would exclusively expand under LIF + 2i and bFGF/Activin culture condition respectively (Fig. 5J). As expected, both GFP and RFP signal from intermediate ESCs was gradually increased under 'LIF only' condition (Additional file 1:Fig. S4A). To contrast, GFP but not RFP signal became readily dominant under LIF + 2i while RFP signal was only marginally affected by bFGF/Activin culture (Additional file 1:Fig. S4B and C). As conversion from the intermediate status to primed ESCs (expressing only RFP+) requires multiple passaging as described previously [42], RFP as well as GFP signal just barely maintained by bFGF/Activin. Of note, iShp2 treatment was likely to interfere in the increase of RFP rather than GFP signal under LIF + 2i (vs. LIF + 2i') and bFGF/Activin (vs. F.A + iShp2) (Fig. 5K, Additional file 16: Movie S5A, Additional file 17: Movie S5B,

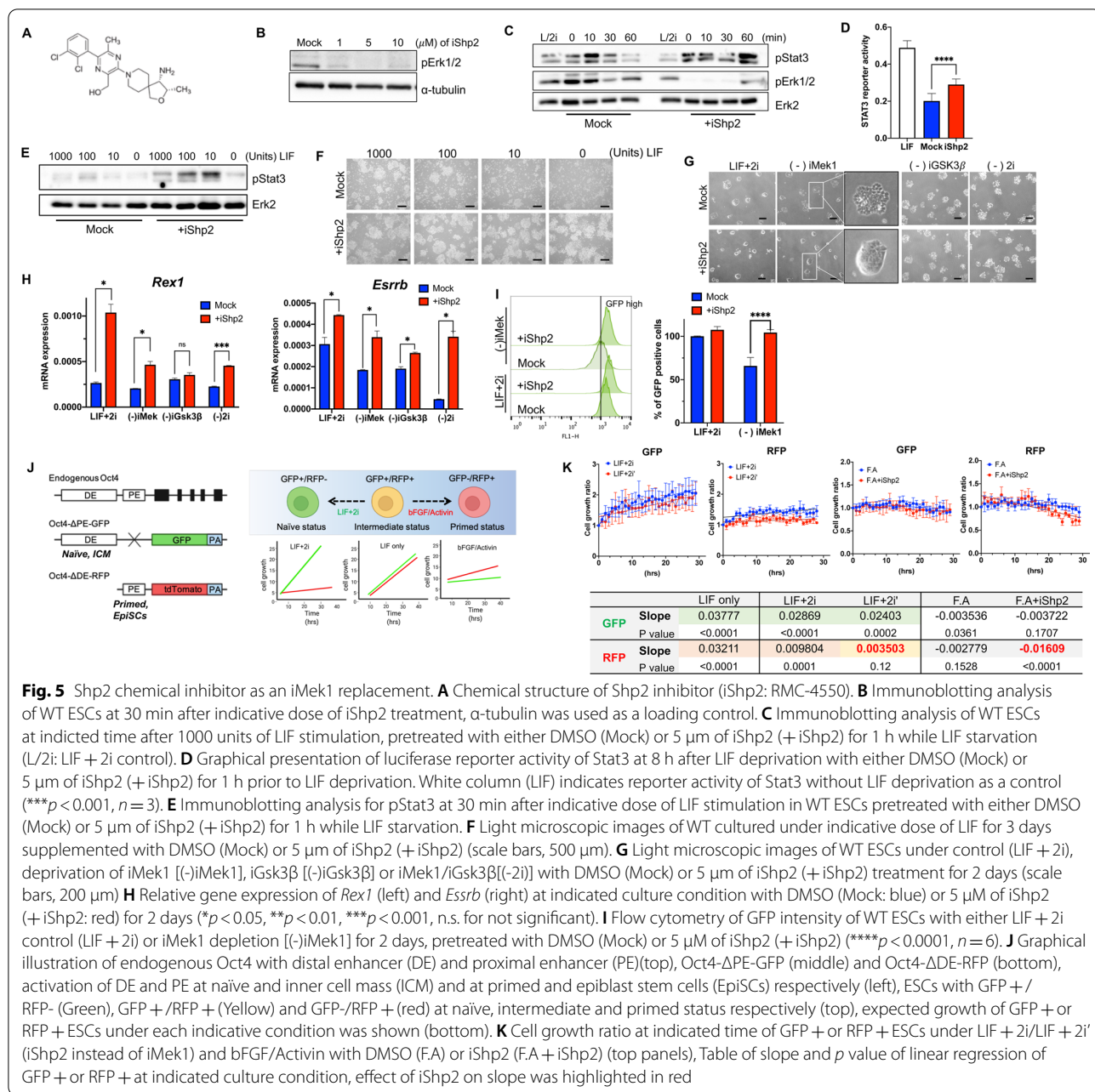
Additional file 18: Movie S5C, Additional file 19: Movie S5D, Additional file 20: Movie S5E), implying that Shp2 inhibition would be unfavorable for ESCs that are under control PE of *Pou5f1*.

## Discussion

The disrupted activity of Shp1 [2] and 2 [26] in mESCs due to a lack of Zap70, a protein that acts as a non-receptor tyrosine kinase upon LIF stimulation, increases Jak/Stat3 signaling and self-renewal. However, although we observed that the effect of Zap70 depletion on hESCs was only marginal unlike mESCs (data not shown), we simply assumed that these discrepancies were largely attributable to species-specific factors and other inherent differences [1]. However, recent advances in the characterization of naïve and primed pluripotency have now revealed that such dissimilarities between mouse and human ESCs result from the unique characteristics of naïve and primed pluripotent stem cells.

Unlike in primed ESCs, the simultaneous chemical inhibition of Mek1 and Gsk3 $\beta$  is critical for the maintenance of naïve pluripotency [9], thus highlighting the unique cellular signaling in the ICM of blastocysts [12, 43]. Particularly, the normal development of Erk2 null





embryos until pre-implantation [44] and low basal Erk activity in ICM [13] suggest that Erk activity is dispensable during the pre-implantation state, which is consistent with the characteristics of naïve pluripotency. Similarly, Shp2 null embryo lethality also results from trophoblast failure [37] and possible epiblast cell death with primed characteristics. To sharp contrast, embryos lacking *Socs3*, another negative regulator of Jak/Stat signaling like Shp2, develop normally till E10.5 and die due to placental abnormality [45], implying marginal effect on early embryogenesis.

The requirement of DUSPs, Erk1/2 specific phosphatases, in mESCs also demonstrates that Erk activity needs to be maintained at a lower level to hold naïve pluripotency [14, 15]. Nevertheless, the constant requirement of the Mek1 inhibitor during in vitro culture of naïve ESCs implies that constant Erk activation occurs due to LIF stimulation, which eventually impedes naïve pluripotency via Erk-dependent phosphorylation [46, 47].

Meta-analysis of previous datasets from a genome-wide study [31] revealed that Shp2 was predicted to serve

as a negative regulator for naïve pluripotency through its involvement in both LIF-Jak/Stat3 and Ras-to-Erk signaling (Fig. 1). Notably, Shp2, whose catalytic activity was induced by LIF along with tyrosyl phosphorylation [18], serves not only as a negative regulator for Stat3 but also as a positive regulator for Ras-to-Erk (Fig. 2). This is why the decoupling of ‘Ras-to-Erk’ signaling occurred through Shp2 inhibition, thus liberating the demand of iMek1 for naïve pluripotency (Fig. 5) as well as enhancing naïve pluripotency (Fig. 2). In sharp contrast, Shp2 appeared to be indispensable for primed ESCs, whose pluripotency relies on bFGF/Activin stimuli. Perturbation of Shp2 significantly delayed the self-renewal of ESCs in primed conditions (Figs. 3 and 5) with concurrent decoupling of Erk signaling (Fig. 3D). Additionally, Shp2 suppression can successfully substitute the usage of iMek1. Therefore, the interfering dual roles of Shp2 with the allosteric inhibitor of Shp2 [21] used in this study prolonged Stat3 activation and attenuated Erk phosphorylation, which mimicked the effect of Shp2 depletion on naïve pluripotency (Fig. 5).

Recently, prolonged usage of iMek1 was demonstrated to cause irreversible changes of (epi)genome, affecting developmental potential [48], which triggers the massive chemical screening for alternatives [49]. Considering the key roles of Shp2 for Erk signaling [16] and successful substitute for iMek1 (Fig. 5), iShp2 would be able to serve as the potential alternative for iMek1 once the effect on status of (epi)genome is determined.

## Conclusions

Shp2 serves as a negative regulator for naïve pluripotency due to its dual roles in Jak/Stat3 and Ras-to-Erk signaling, whereas the pluripotency of primed cells depended on bFGF/Activin, which could also be modulated by Shp2-dependent signaling. Allosteric inhibition of Shp2 with an inhibitor to disrupt these dual functions can therefore be used to improve naïve pluripotency and replace the use of iMek1. Considering the complex protocol for human naïve pluripotent stem cell conversion [50], iShp2 treatment would be a promising strategy for the efficient establishment of human naïve PSCs, which will be examined in future studies.

## Materials and methods

### Reagents

The primary antibodies against  $\alpha$ -tubulin (#sc-8035),  $\beta$ -actin (#sc-47778), Stat3 (#sc-8019), Erk2 (#sc-154) were purchased from Santa Cruz Biotechnology, Inc. Antibodies against phospho-Shp2 (Tyr542) (#3751), phospho-Stat3 (#9145s), phospho-Erk1/2 (#9101), phospho-Mek1/2 (#9121s) were purchased from Cell Signaling Technology. Antibodies against Shp2 (#PA5-95069)

and phospho-Src (#44660 g) were purchased from Invitrogen. The secondary antibodies against mouse IgG (#115-035-003) and rabbit IgG (#111-035-003) were purchased from Jackson ImmunoResearch Laboratories, Inc. siRNAs targeting Negative Control (#SN-1003) and the others were obtained from Bioneer. Expression vectors of  $6 \times$  Stat3-luciferase was kindly gifted by Prof. Hyewon Youn from Seoul National University.

### Cell culture

Naïve mouse ESCs were cultured on 0.5% porcine gelatin-coated dish in Naïve mESC culture media -DMEM high glucose (Gibco) supplemented with 15% FBS (Gibco), 1% Glutamax (Gibco), 1% MEM-nonessential amino acids (Gibco), 0.1% Gentamycin (Gibco), 0.1 mM  $\beta$ -mercaptoethanol (Gibco), 1,000 U/ml mouse leukemia inhibitory factor (mLIF) (Millipore, Merck), 1  $\mu$ m PD0325901 (Peprotech) and 3  $\mu$ m CHIR99021- at 37 °C and 5% CO<sub>2</sub> incubating condition. Cells were passaged 1:20 ratio every 3 days using 0.25% Trypsin/EDTA (Wellgene) as a single cell dissociation reagent. Primed mouse ESCs were cultured on Matrigel (Corning# 354277)-coated dish in EpiSC culture media -DMEM/F12 (Gibco) supplemented with 15% KnockOut SR (Gibco), 1% GlutaMAX (Gibco), 1% MEM-nonessential amino acids (Gibco), 0.1% Gentamycin (Gibco), 10 ng/ml murine bFgf (Peprotech), 20 ng/ml murine Activin (Peprotech)- at 37 °C and 5% CO<sub>2</sub> condition. Primed mESCs were passaged every 3–4 days using Dispase (Gibco) as a colony detachment reagent. Detached colony clumps were transferred 1:15–1:20 ratio on Matrigel (Corning# 354277) coated dishes. Culture media was changed every day for all cell lines. Oct4- $\Delta$ PPE-GFP/ $\Delta$ DE-RFP ESCs were cultured on mitogen-inactivated C57BL/6 feeder cells on 0.15% porcine gelatin-coated dish in culture media-DMEM Low (Gibco) supplemented with 15% FBS (Gibco), 1% P.S.G (Gibco), 1% MEM-nonessential amino acids (Gibco), 0.1 mM  $\beta$ -mercaptoethanol (Gibco) and 1000 U/ml mouse leukemia inhibitory factor (mLIF) (Millipore, Merck)- at 37 °C and 5% CO<sub>2</sub> incubating condition.

### Teratoma formation assay

$5 \times 10^5$  cells of each OG2 and OG2Shp2KD mESCs were injected into the testes of 5-weeks-old male BALB/C nude mice ( $n=3$ ), and subcutaneously injected in the neck ( $n=5$ ) and abdomen ( $n=5$ ) of 5-weeks-old male BALB/C nude mice. Mice were euthanized 6 weeks after the injection. Animal experiments were conducted under the permission of Seoul National University Institutional Animal Care and Use Committee (Permission number: SNU-190716–5-2).

### RNA-sequencing analysis

Total RNA was isolated from cell pellets by using Easy-BLUE™ RNA isolation kit (iNtRON Biotechnology). 1 mg of total RNA was processed for preparing mRNA sequencing library using MGI Easy RNA Directional Library Prep Kit (MGI) following manufacturer's instruction. The mRNA is fragmented into small pieces under elevated temperature. The cleaved RNA fragments are copied into first strand cDNA using reverse transcriptase and random primers. Strand specificity is achieved in the RT directional buffer and second strand cDNA synthesis was done. Single 'A' base was added to the cDNA fragments, followed by ligation of the adapter. The products are purified and enriched by PCR procedure to acquire the final cDNA library. The cDNA library is quantified using QuantiFluor ONE dsDNA System (Promega). Using DNA nanoball (DNB) enzyme, the library is incubated at 30 °C for 25 min to make DNB. Finally, sequencing of the prepared DNB was performed using MGIseq system (MGI) with 100 bp paired-end reads.

### Establishment of Shp2KD cell line

Shp2 stable knocked-down cell line was acquired by introducing shPtpn11 Piggy-Bac vector and Transposase vector. Transfection was performed using Lipofectamine 3000 reagent (#L3000-001, Invitrogen). G418 selection (600 µg/ml) was done for 9 days. Single colony selection was performed from heterogenous Shp2KD pool cells.

### Flow cytometric analysis

GFP intensity of OG2 cells were measured by Flow cytometric analysis. Cells were dissociated with Accutase (#561527, BD Bio-sciences) and washed three times with DPBS. Cells were analyzed through FACS Carlibur (BD Bioscience). GFP intensity was determined by measuring FITC channel.

### Live cell imaging

Brightfield images and GFP images of cells on specific area were captured every hour by JuLi Stage (NanoEntek). Acquired images were merged to create time-lapse cell history movies using JuLi-Edit. Relative fluorescence intensity and area of acquired images were measured by using the ImageJ analysis program (ImageJ bundled with ZuluOpen JDK 13.0.6 version, National Institutes of Health, Bethesda, MD, USA; <https://imagej.nih.gov/ij>).

### Cell tracing

Cell tracing was performed with CellTrace™ Far Red Cell Proliferation Kit (Invitrogen). Cells were pre-treated with CellTrace™ Far Red reagent (1:1000) for 24 h. Both Far

Red-labeled and unlabeled cells were mixed 1:1 ratio and co-cultured. Fluorescence images of live cell was acquired by JuLi Stage (NanoEntek).

### RNA isolation and quantitative RT-PCR analysis

Total RNA was isolated from cells using Easy-Blue™ total RNA isolation kit (iNtRON Biotech) following the manufacturer's instructions. 5 × PrimeScript™ RT mix (TaKaRa) was used during reverse transcription to acquire cDNA. Quantitative real-time PCR was performed using 2 × TB-Green premix (TaKaRa) by LightCycler-480®II (Roche). *Rn18s* gene was used as internal loading control for normalizing gene expression data (Table 1).

### Dual luciferase reporter assay

Cells were co-transfected with 6×Stat3 reporter vector and pRL vector using Lipofectamine 2000 reagent (#11668019, Invitrogen). After 3 h of incubation with 1 × passive lysis buffer followed by centrifugation, supernatant from the cell lysate was acquired. The supernatant was used for the reaction with LARII and Stop & Glo reagent. Stat3 luciferase assay was performed using Dual Luciferase Reporter Assay System Kit (#E1980, Promega), and detected by SpectraMax® i3x Multi-Mode Microplate Reader.

### Phosphatase activity assay

Shp2 phosphatase activity was carried out with PTP assay kit 1 (#17-125, Sigma-Aldrich) according to the manufacturer's protocol. In brief, 10 mM of p-nitrophenylphosphate (pNPP), used as the substrate for phosphatase activity assay was incubated at 30 °C for 30 min under assay buffer (30 mM HEPES at pH 7.4, 120 mM NaCl, 5 mM DTT). The relative optical density was determined by 405 nm absorbance using Epoch (BioTek).

### Immunoblotting analysis

Whole Cell lysate was extracted using RIPA buffer (Biosesang), supplemented with 1 µM protease inhibitor, 10 µM sodium orthovanadate. After 1 h incubation on ice followed by centrifugation, whole cell lysate was acquired. Quantification of proteins were performed with pierce BCA protein assay Kit (#23225, Thermo Fischer Scientific). Protein sample was prepared by adding 5 × SDS-PAGE loading buffer (#SF2088-110-00, Biosesang) and boiling at 100 °C for 10 min. Approximately 15 µg of each total protein was loaded and separated on 10% SDS-PAGE gel. Separated proteins were transferred to activated PVDF membrane. Membrane with transferred proteins was blocked with 5% skim milk in TBS-T in RT for 1 h followed by washing. Primary antibody (1:500 ~ 1:1000) in TBS-T was incubated with 1% sodium

azide at 4 °C for overnight. After washing, the membrane was incubated with secondary antibody (1:10000) in TBS-T at RT for 1 h. Chemoluminescence was detected by Chemi-Doc using Miracle-Star (#16028, iNtRON Biotechnology) kit or West-Queen (#16026, iNtRON Biotechnology) kit.

### Immunoprecipitation

Cell lysate was extracted using RIPA buffer (Biosesang), (1 μM protease inhibitor, 10 μM sodium orthovanadate). After 1 h incubation on ice followed by centrifugation, whole cell lysate was acquired. 1 μg of Shp2 antibody (#VL3159027A, Invitrogen) was added in protein lysate and incubated at 4 °C for overnight. Protein A agarose (#sc-2001, Santa-cruz) was added in protein lysate and incubated at 4 °C for 4 h. Beads were gathered by centrifugation and protein sample was prepared by adding 5 × SDS-PAGE loading buffer (#SF2088-110-00, Biosesang), followed by boiling at 100 °C for 10 min.

### Gene set enrichment analysis (GSEA)

FPKM values of RNA sequencing data were formatted and loaded to run Gene Set Enrichment Analysis. GSEA software and the Gene Sets (Hallmark\_IL6\_JAK\_STAT3 signaling, KEGG\_JAK\_STAT3 signaling, ABBUD\_LIF signaling\_up, Hallmark\_KRAS\_signaling\_DN, Hallmark\_KRAS\_signaling\_UP) were downloaded from Molecular Signatures Database v7.4 (<https://www.gsea-msigdb.org>).

### Statistical analysis

The quantitative data are presented as the mean values ± standard deviation (SD). Unpaired two-tailed *t*-tests or one-way ANOVA following Dunnett multiple comparison, was performed to analyze the statistical significance of each response variable. *p*-values less than 0.05 were considered statistically significant (\* < 0.05, \*\* < 0.01, \*\*\* < 0.001, \*\*\*\* < 0.0001 and n.s. for not significant).

### Supplementary Information

The online version contains supplementary material available at <https://doi.org/10.1186/s13287-022-02976-z>.

**Additional file 1:** Supplementary Figures 1-4, Supplementary Figure legends, Supplementary Movie legends.

**Additional file 2: Movie S1A.** Fluorescence microscopic live images of WT ESCs under LIF+2i condition (Figure S1A).

**Additional file 3: Movie S1B.** Fluorescence microscopic live images of WT ESCs under LIF only condition (Figure S1A).

**Additional file 4: Movie S1C.** Fluorescence microscopic live images of WT ESCs under LIF- condition (Figure S1A).

**Additional file 5: Movie S2A.** Fluorescence microscopic live images of WT ESCs under LIF+2i condition (Figure 2D).

**Additional file 6: Movie S2B.** Fluorescence microscopic live images of KD ESCs under LIF+2i condition (Figure 2D).

**Additional file 7: Movie S2C.** Fluorescence microscopic live images of WT ESCs under LIF only condition (Figure 2D).

**Additional file 8: Movie S2D.** Fluorescence microscopic live images of KD ESCs under LIF only condition (Figure 2D).

**Additional file 9: Table S1.** Gene lists of regulators for naïve pluripotency (Figure S1C).

**Additional file 10: Movie S3A.** Light microscopic live images of WT under LIF+2i condition (Figure 3A).

**Additional file 11: Movie S3B.** Light microscopic live images of WT under bFGF/Activin condition (Figure 3A).

**Additional file 12: Movie S3C.** Light microscopic live images of KD under LIF+2i condition (Figure 3A).

**Additional file 13: Movie S3D.** Light microscopic live images of KD under bFGF/Activin condition (Figure 3A).

**Additional file 14: Movie S4A.** Fluorescence microscopic live images of co-cultured WT and KD ESCs under LIF+2i condition (Figure 3C).

**Additional file 15: Movie S4B.** Fluorescence microscopic live images of co-cultured WT and KD ESCs under bFGF/Activin condition (Figure 3C).

**Additional file 16: Movie S5A.** Fluorescence microscopic live images of GFP and RFP under LIF only condition (Figure S4A).

**Additional file 17: Movie S5B.** Fluorescence microscopic live images of GFP and RFP under LIF+2i condition (Figure S4B, S4C).

**Additional file 18: Movie S5C.** Fluorescence microscopic live images of GFP and RFP under LIF+2i' condition (Figure S4B, S4C).

**Additional file 19: Movie S5D.** Fluorescence microscopic live images of GFP and RFP under bFGF/Activin condition (Figure S4B, S4C).

**Additional file 20: Movie S5E.** Fluorescence microscopic live images of GFP and RFP under bFGF/Activin +iShp2 condition (Figure S4B, S4C).

### Acknowledgements

This work was supported by a grant from the National Research Foundation of Korea (NRF-2020R1A2C2005914). This work was also supported by the Creative-Pioneering Researchers Program through Seoul National University (SNU).

### Author contributions

HJC and KTK conceived the overall study design and led the experiments. SMK mainly conducted the experiments, data analysis, and critical discussion of the results. EJK performed RNAseq data analysis, YJK, YHK, JYO, SP and JTD produced mutant lines and provided key cell line systems. All authors have read and approved the manuscript.

### Availability of data and materials

Source data are available from the corresponding authors upon request.

### Declarations

#### Ethics approval and consent to participate

Not applicable.

#### Consent for publication

This manuscript does not contain data from any individual person.

#### Competing of interests

The authors declare that they have no known competing financial interests or personal relationships that could have appeared to influence the work reported in this paper.

#### Author details

<sup>1</sup>College of Pharmacy, Seoul National University, 1 Gwanak-ro Gwanak-gu, Seoul 08826, Republic of Korea. <sup>2</sup>Research Institute of Pharmaceutical Sciences, Seoul National University, Seoul, Republic of Korea. <sup>3</sup>Department of Biomedical Sciences, Seoul National University College of Medicine, Seoul, South



Korea. <sup>4</sup>Department of Stem Cell and Regenerative Biology, College of Animal Bioscience and Technology, Konkuk University, Seoul, Republic of Korea.

Received: 7 October 2021 Accepted: 17 June 2022

Published online: 18 July 2022

## References

- Ginis I, Luo Y, Miura T, Thies S, Brandenberger R, Gerecht-Nir S, Amit M, Hoke A, Carpenter MK, Itskovitz-Eldor J, et al. Differences between human and mouse embryonic stem cells. *Dev Biol.* 2004;269(2):360–80.
- Cha Y, Moon BH, Lee MO, Ahn HJ, Lee HJ, Lee KA, Fornace AJ Jr, Kim KS, Cha HJ, Park KS. Zap70 functions to maintain stemness of mouse embryonic stem cells by negatively regulating Jak1/Stat3/c-Myc signaling. *Stem cells.* 2010;28(9):1476–86.
- Jeong HC, Park SJ, Choi JJ, Go YH, Hong SK, Kwon OS, Shin JG, Kim RK, Lee MO, Lee SJ, et al. PRMT8 Controls the pluripotency and mesodermal fate of human embryonic stem cells by enhancing the PI3K/AKT/SOX2 axis. *Stem cells.* 2017;35(9):2037–49.
- Cha Y, Han MJ, Cha HJ, Zoldan J, Burkart A, Jung JH, Jang Y, Kim CH, Jeong HC, Kim BG, et al. Metabolic control of primed human pluripotent stem cell fate and function by the miR-200c-SIRT2 axis. *Nat Cell Biol.* 2017;19(5):445–56.
- Martello G, Smith A. The nature of embryonic stem cells. *Annu Rev Cell Dev Biol.* 2014;30:647–75.
- Nichols J, Smith A. Naive and primed pluripotent states. *Cell Stem Cell.* 2009;4(6):487–92.
- Hanna J, Cheng AW, Saha K, Kim J, Lengner CJ, Soldner F, Cassady JP, Muffat J, Carey BW, Jaenisch R. Human embryonic stem cells with biological and epigenetic characteristics similar to those of mouse ESCs. *Proc Natl Acad Sci U S A.* 2010;107(20):9222–7.
- Weinberger L, Ayyash M, Novershtern N, Hanna JH. Dynamic stem cell states: naive to primed pluripotency in rodents and humans. *Nat Rev Mol Cell Biol.* 2016;17(3):155–69.
- Ying QL, Wray J, Nichols J, Battle-Morera L, Doble B, Woodgett J, Cohen P, Smith A. The ground state of embryonic stem cell self-renewal. *Nature.* 2008;453(7194):519–23.
- Niwa H, Burdon T, Chambers I, Smith A. Self-renewal of pluripotent embryonic stem cells is mediated via activation of STAT3. *Genes Dev.* 1998;12(13):2048–60.
- Cheng JG, Chen JR, Hernandez L, Alvord WG, Stewart CL. Dual control of LIF expression and LIF receptor function regulate Stat3 activation at the onset of uterine receptivity and embryo implantation. *Proc Natl Acad Sci USA.* 2001;98(15):8680–5.
- Huyghe A, Furlan G, Ozmadenci D, Galonska C, Charlton J, Gaume X, Combemorel N, Riemenschneider C, Allegre N, Zhang J, et al. Netrin-1 promotes naive pluripotency through Neol1 and Unc5b co-regulation of Wnt and MAPK signalling. *Nat Cell Biol.* 2020;22(4):389–400.
- Simon CS, Rahman S, Raina D, Schroter C, Hadjantonakis AK. Live visualization of ERK activity in the mouse blastocyst reveals lineage-specific signaling dynamics. *Dev Cell.* 2020;55(3):341–53.
- Chappell J, Sun Y, Singh A, Dalton S. MYC/MAX control ERK signaling and pluripotency by regulation of dual-specificity phosphatases 2 and 7. *Genes Dev.* 2013;27(7):725–33.
- Li Z, Fei T, Zhang J, Zhu G, Wang L, Lu D, Chi X, Teng Y, Hou N, Yang X, et al. BMP4 Signaling Acts via dual-specificity phosphatase 9 to control ERK activity in mouse embryonic stem cells. *Cell Stem Cell.* 2012;10(2):171–82.
- Dance M, Montagner A, Salles JP, Yart A, Raynal P. The molecular functions of Shp2 in the Ras/Mitogen-activated protein kinase (ERK1/2) pathway. *Cell Signal.* 2008;20(3):453–9.
- Feng GS. Shp2-mediated molecular signaling in control of embryonic stem cell self-renewal and differentiation. *Cell Res.* 2007;17(1):37–41.
- Lu W, Gong D, Bar-Sagi D, Cole PA. Site-specific incorporation of a phosphotyrosine mimetic reveals a role for tyrosine phosphorylation of SHP-2 in cell signaling. *Mol Cell.* 2001;8(4):759–69.
- Mohi MG, Neel BG. The role of Shp2 (PTPN11) in cancer. *Curr Opin Genet Dev.* 2007;17(1):23–30.
- Cunnick JM, Dorsey JF, Munoz-Antonia T, Mei L, Wu J. Requirement of SHP2 binding to Grb2-associated binder-1 for mitogen-activated protein kinase activation in response to lysophosphatidic acid and epidermal growth factor. *J Biol Chem.* 2000;275(18):13842–8.
- Nichols RJ, Haderk F, Stahlhut C, Schulze CJ, Hemmati G, Wildes D, Tzitzilonis C, Mordec K, Marquez A, Romero J, et al. RAS nucleotide cycling underlies the SHP2 phosphatase dependence of mutant BRAF-, NF1- and RAS-driven cancers. *Nat Cell Biol.* 2018;20(9):1064–73.
- Ruess DA, Heynen GJ, Ciecieski KJ, Ai J, Berninger A, Kabacaoglu D, Gorgulu K, Dantes Z, Wormann SM, Diakopoulos KN, et al. Mutant KRAS-driven cancers depend on PTPN11/SHP2 phosphatase. *Nat Med.* 2018;24(7):954–60.
- Fedele C, Ran H, Diskin B, Wei W, Jen J, Geer MJ, Araki K, Ozerdem U, Simeone DM, Miller G, et al. SHP2 Inhibition Prevents Adaptive Resistance to MEK Inhibitors in Multiple Cancer Models. *Cancer Discov.* 2018;8(10):1237–49.
- Chen YN, LaMarche MJ, Chan HM, Fekkes P, Garcia-Fortanet J, Acker MG, Antonakos B, Chen CH, Chen Z, Cooke VG, et al. Allosteric inhibition of SHP2 phosphatase inhibits cancers driven by receptor tyrosine kinases. *Nature.* 2016;535(7610):148–52.
- Burdon T, Tracey C, Chambers I, Nichols J, Smith A. Suppression of SHP-2 and ERK signalling promotes self-renewal of mouse embryonic stem cells. *Dev Biol.* 1999;210(1):30–43.
- Cha Y, Park KS. SHP2 is a downstream target of ZAP70 to regulate JAK1/STAT3 and ERK signaling pathways in mouse embryonic stem cells. *FEBS Lett.* 2010;584(19):4241–6.
- Wu D, Pang Y, Ke Y, Yu J, He Z, Tautz L, Mustelin T, Ding S, Huang Z, Feng GS. A conserved mechanism for control of human and mouse embryonic stem cell pluripotency and differentiation by shp2 tyrosine phosphatase. *PLoS ONE.* 2009;4(3):e4914.
- Yoshimizu T, Sugiyama N, De Felice M, Yeom YI, Ohbo K, Masuko K, Obinata M, Abe K, Scholer HR, Matsui Y. Germline-specific expression of the Oct-4/green fluorescent protein (GFP) transgene in mice. *Dev Growth Differ.* 1999;41(6):675–84.
- Cho SJ, Kim KT, Kim JS, Kwon OS, Go YH, Kang NY, Heo H, Kim MR, Han DW, Moon SH, et al. A fluorescent chemical probe CDy9 selectively stains and enables the isolation of live naive mouse embryonic stem cells. *Biomaterials.* 2018;180:12–23.
- Chen W, Daines MO, Khurana Hershey GK. Turning off signal transducer and activator of transcription (STAT): the negative regulation of STAT signaling. *J Allergy Clin Immunol.* 2004;114(3):476–89.
- Li M, Yu JSL, Tilgner K, Ong SH, Koike-Yusa H, Yusa K. Genome-wide CRISPR-KO screen uncovers mTORC1-mediated Gsk3 regulation in naive pluripotency maintenance and dissolution. *Cell Rep.* 2018;24(2):489–502.
- Liberzon A, Subramanian A, Pinchback R, Thorvaldsdottir H, Tamayo P, Mesirov JP. Molecular signatures database (MSigDB) 3.0. *Bioinformatics.* 2011;27(12):1739–40.
- Lehmann U, Schmitz J, Weissenbach M, Sobota RM, Hortner M, Friederichs K, Behrmann I, Tsiaris W, Sasaki A, Schneider-Mergener J, et al. SHP2 and SOCS3 contribute to Tyr-759-dependent attenuation of interleukin-6 signaling through gp130. *J Biol Chem.* 2003;278(1):661–71.
- Bennett AM, Tang TL, Sugimoto S, Walsh CT, Neel BG. Protein-tyrosine-phosphatase SHPTP2 couples platelet-derived growth factor receptor beta to Ras. *Proc Natl Acad Sci U S A.* 1994;91(15):7335–9.
- Gadient RA, Patterson PH. Leukemia inhibitory factor, Interleukin 6, and other cytokines using the GP130 transducing receptor: roles in inflammation and injury. *Stem cells.* 1999;17(3):127–37.
- Subramanian A, Tamayo P, Mootha VK, Mukherjee S, Ebert BL, Gillette MA, Paulovich A, Pomeroy SL, Golub TR, Lander ES, et al. Gene set enrichment analysis: a knowledge-based approach for interpreting genome-wide expression profiles. *Proc Natl Acad Sci USA.* 2005;102(43):15545–50.
- Yang W, Klamann LD, Chen B, Araki T, Harada H, Thomas SM, George EL, Neel BG. An Shp2/SFK/Ras/Erk signaling pathway controls trophoblast stem cell survival. *Dev Cell.* 2006;10(3):317–27.
- Greber B, Wu G, Bernemann C, Joo JY, Han DW, Ko K, Tapia N, Sabour D, Sternecker J, Tesar P, et al. Conserved and divergent roles of FGF signaling in mouse epiblast stem cells and human embryonic stem cells. *Cell Stem Cell.* 2010;6(3):215–26.
- Saxton TM, Henkemeyer M, Gasca S, Shen R, Rossi DJ, Shalaby F, Feng GS, Pawson T. Abnormal mesoderm patterning in mouse embryos mutant for the SH2 tyrosine phosphatase Shp-2. *EMBO J.* 1997;16(9):2352–64.
- O'Reilly AM, Neel BG. Structural determinants of SHP-2 function and specificity in *Xenopus* mesoderm induction. *Mol Cell Biol.* 1998;18(1):161–77.

41. Ahmed TA, Adamopoulos C, Karoulia Z, Wu X, Sachidanandam R, Aaronson SA, Poulidakos PI. SHP2 drives adaptive resistance to ERK signaling inhibition in molecularly defined subsets of ERK-dependent tumors. *Cell Rep*. 2019;26(1):65–78.
42. Choi HW, Joo JY, Hong YJ, Kim JS, Song H, Lee JW, Wu G, Scholer HR, Do JT. Distinct enhancer activity of Oct4 in naive and primed mouse pluripotency. *Stem cell Rep*. 2016;7(5):911–26.
43. Azami T, Bassalart C, Allegre N, Valverde Estrella L, Pouchin P, Ema M, Chazaud C. Regulation of the ERK signalling pathway in the developing mouse blastocyst. *Development*. 2019;146(14):dev177139.
44. Saba-El-Leil MK, Vella FD, Vernay B, Voisin L, Chen L, Labrecque N, Ang SL, Meloche S. An essential function of the mitogen-activated protein kinase Erk2 in mouse trophoblast development. *EMBO Rep*. 2003;4(10):964–8.
45. Roberts AW, Robb L, Rakar S, Hartley L, Cluse L, Nicola NA, Metcalf D, Hilton DJ, Alexander WS. Placental defects and embryonic lethality in mice lacking suppressor of cytokine signaling 3. *Proc Natl Acad Sci USA*. 2001;98(16):9324–9.
46. Kim MO, Kim SH, Cho YY, Nadas J, Jeong CH, Yao K, Kim DJ, Yu DH, Keum YS, Lee KY, et al. ERK1 and ERK2 regulate embryonic stem cell self-renewal through phosphorylation of Klf4. *Nat Struct Mol Biol*. 2012;19(3):283–90.
47. Kim SH, Kim MO, Cho YY, Yao K, Kim DJ, Jeong CH, Yu DH, Bae KB, Cho EJ, Jung SK, et al. ERK1 phosphorylates Nanog to regulate protein stability and stem cell self-renewal. *Stem Cell Res*. 2014;13(1):1–11.
48. Choi J, Huebner AJ, Clement K, Walsh RM, Savol A, Lin K, Gu H, Di Stefano B, Brumbaugh J, Kim SY, et al. Prolonged Mek1/2 suppression impairs the developmental potential of embryonic stem cells. *Nature*. 2017;548(7666):219–23.
49. Khan SA, Park KM, Fischer LA, Dong C, Lungjangwa T, Jimenez M, Casalena D, Chew B, Dietmann S, Auld DS, et al. Probing the signaling requirements for naive human pluripotency by high-throughput chemical screening. *Cell Rep*. 2021;35(11):109233.
50. Theunissen TW, Friedli M, He Y, Planet E, O'Neil RC, Markoulaki S, Pontis J, Wang H, Iouranova A, Imbeault M, et al. Molecular criteria for defining the naive human pluripotent state. *Cell Stem Cell*. 2016;19(4):502–15.

## Publisher's Note

Springer Nature remains neutral with regard to jurisdictional claims in published maps and institutional affiliations.

Ready to submit your research? Choose BMC and benefit from:

- fast, convenient online submission
- thorough peer review by experienced researchers in your field
- rapid publication on acceptance
- support for research data, including large and complex data types
- gold Open Access which fosters wider collaboration and increased citations
- maximum visibility for your research: over 100M website views per year

At BMC, research is always in progress.

Learn more [biomedcentral.com/submissions](https://biomedcentral.com/submissions)

